# Dynamic Topology Inference via External Observation for Multi-Robot Formation Control

Cong Liu, Jianping He, Shanying Zhu and Cailian Chen

*Abstract*—**Network communication topology through which robots achieve intelligent collaboration in multi-robot formation control systems is of fundamental importance. Existing works focusing on security issues of multi-robot systems usually assume that the topology is priori knowledge. However, the topology graph is not accessible for inner security policies or ID identification from the outside of the system. An intriguing question is how to construct the communication topology via observation from the outside point of view. This work studies the problem of constructing topology graph that represents magnitude of robots interaction via observing trajectories. The main novelties of this work include: i) It is the first time to consider the topology inference problem in multi-robot formation control systems. ii) We transform the inference issue into a linear regression problem. The optimal estimation of Perron matrix that contains the interaction profile is derived using $l_2$-norm least square algorithm ($l_2$-LS). iii) Considering the link failure and creation, we propose a novel dynamic window least square algorithm (DWLS) to identify dynamic changing topology. Finally, simulation results demonstrate that $l_2$-LS has $95\%$ inference accuracy averagely when noise parameter $\mu = 0.05$, and DWLS is robust and stable in identifying time slices, moreover, accuracy approaches $90\%$.**

## I. Introduction

Over the past decades, multi-robot formation control systems have been extensively investigated for their various applications and theoretical challenges [1] [2]. Formation control, as the key spot of the multi-robot control system, has been discussed and developed. Typical formation control methods include consensus-based, leader-follower and virtual structure [3], [4]. In these methods, consensus-based formation tracking algorithm is the most widely used algorithm, where each robot decides the next motion autonomously under a discrete time dynamic and they finally gather to form a formation and achieve an agreement.

However, most of the existing works focus on designing formation control algorithms for better stability and robustness. When security issue is concerned, a more intriguing problem is how to reconstruct the topology of connected robots via observation, since the attacker can use the topology information as the knowledge and apply intelligent attack scheme [5]. For example, the attacker can search the leader node of the topology and launch precision attack with the least cost. This issue is full of challenges but meaningful in both theory research and real applications [6]–[9].

In essence, topology inference via observation is an inverse problem from pure mathematical view. For multi-robot formation control systems, inferring its topology involves some challenges in practice. First, observed data within sufficient long horizon which contains enough correlation information of the states between robots is necessary. Besides, there are continuous random noises during observation and the precision of sensors is limited, making the problem less tractable.

This type of problem arises in many domains and we are inspired by some existing works. For example, [10] studies the network topology's influence on the outbreak of diseases. In brain network, interactions among neurons are significant and they might improve the understanding of the disease [11], [12]. From a merely theoretical perspective, these problems fall under the umbrella of signal processing over graphs [13], [14]. The aforementioned research emphasizes the graph signal processing problem in various domains, which has the similar mechanism as multi-robot formation control systems.

There are some works which investigate topology inference problem for different system models. In [15], the topology inference for linear stochastic dynamic systems is discussed. In [16], [17], the problem in casual dynamics model focus on learning the causal relationships by means of functional dependencies. [18] addresses the problem of learning Laplacians, which is equivalent to learning graph topologies. However, this work focus on a new proposed representation model for smooth graph signals based on the extension of the traditional factor analysis model. [19] proposes a characterization of the space of valid graphs to realize the graph recovery, in the sense that they can explain stationary signals. [20] addresses the problem of inferring a graph structure from the observation of signals. The most related literature [13] aims at reconstructing the interaction profile of the observable portion of the network. The estimated accuracy is affected by distribution of random noise and other factors like noise accumulation caused by dynamics, observation capability or resolution. Therefore, it is of great interest to propose new analysis approaches to guarantee higher inference accuracy. The main contributions of this paper are summarized as follows:

- To the best of our knowledge, this is the first time to consider the topology inference problem of multi-robot formation control systems via external observation, which requires no prior knowledge of system dynamics.
- We propose an effective reconstruction algorithm $l_2$-LS,

The authors are with the Department of Automation, Shanghai Jiao Tong University, and Key Laboratory of System Control and Signal Processing, Ministry of Education of China, Shanghai 200240, China. E-mail: sjtu2017@sjtu.edu.cn, jphe@sjtu.edu.cn, cailianchen@sjtu.edu.cn. This work is partially sponsored by the National Key R&D Program of China 2017YFE0114600, NSFC of china under grant 61622307, 61603251 and NSF of Shanghai Municipality under grant 18ZR1419900.

978-1-7281-2794-1/19/$31.00 ©2019 IEEE

which transforms the topology inference issue into a linear regression problem. Then, the optimal estimation of Perron matrix that represents the topology is derived.

- To deal with the topology inference problem under the impact of network uncertainties, e.g. packet loss, we consider the dynamic topology case. We then propose DWLS algorithm based on $l_2$-LS.
- Numerical simulations are conducted to illustrate the effectiveness and feasibility of the proposed algorithms.

The remainder of this paper is organized as follows. In Section II, formation control model and problem description are introduced. In section III, $l_2$-LS and DWLS are proposed. Simulation are shown in Section IV and Section V concludes.

## II. Preliminaries and Problem Formulation

### A. Network Model

Communication among agents is modeled as an directed graph $\mathcal{G}=(\mathcal{V},\mathcal{E})$, where $\mathcal{V}$ is the finite set of nodes $\mathcal{V}=\{v_1,\cdots,v_N\}$ and $\mathcal{E}\in\mathcal{V}\times\mathcal{V}$ denotes the set of edges connecting two nodes. The neighbor set of robot node $i$ is denoted by $N_i$, where $j\in N_i$ if and only if the link $(v_i,v_j)\in\mathcal{E}$. The adjacency matrix $A=[a_{ij}]\in\mathbb{R}^{N\times N}$ of a graph is defined such that $a_{ij}=1$ when $(v_i,v_j)\in\mathcal{E}$ and $a_{ij}=0$ otherwise. $a_{ij}=1$ means the robot node $i$ updates its next state with the combination of node $j$'s information. The specific adjacency matrix $A$ corresponds to a unique topology $\mathcal{G}(A)$. The Laplacian matrix of graph $\mathcal{G}$ is defined as $\mathcal{L}=[l_{ij}]\in\mathbb{R}^{N\times N}$ with $l_{ii}=\sum_{j=1,j\neq i}^{N}a_{ij}$ and $l_{ij}=-a_{ij},i\neq j$.

### B. Formation Control of Mobile Robots

Assume that there are $N$ robots on a two-dimensional plane. The states of each robot satisfies single-integrator kinematics,

$$\dot{p}_i=u_i,\ \ i\in\{1,2,\cdots,N\}, \tag{1}$$

where $p_i=[x_i\ y_i]^T, u_i=[u_{ix}\ u_{iy}]^T\in\mathbb{R}^2$ are position vector and control input of robot $i$, respectively. Define the formation distance $\Delta_i=[\Delta_{ix},\Delta_{iy}]$, which is robot $i$-th desired position relative to the leader (leader leads the formation and followers take the leader as the formation reference).

We assume that the leader's in-degree is zero which means leader's update equation contains no information from other robot nodes. The leader's desired trajectory is realized by the control law $u_i=f(t,p_0)$. For the simplicity of presentation, we study one-dimensional space. However, results are still valid for the high-dimensional space by the introduction of the Kronecker product.

To realize the formation tracking, we adopt the following distributed consensus algorithm in follower robots

$$u_i=\sum_{i\in N_i}\varepsilon a_{ij}((p_j-p_i)-(\Delta_j-\Delta_i)), \tag{2}$$

the non-negative $\varepsilon$ is an admissible time-step which determines the convergence speed of formation forming. In x-axis, robot $i$-th discrete-time dynamic is as follows

$$x_i(t_{k+1})=x_i(t_k)+u_i(t_k),k=0,1,\cdots,n, \tag{3}$$

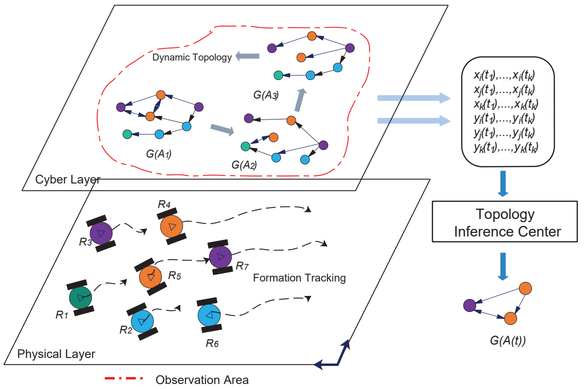


Fig. 1: Illustration of topology inference problem.

combining $N$ linear combination equations in (2) and (3) for all the robots, the global dynamics are given by

$$\begin{aligned}x(t_{k+1})&=(I_N-\varepsilon\mathcal{L})x(t_k)+\varepsilon\mathcal{L}\Delta_x\\&=Px(t_k)+b_x,\end{aligned} \tag{4}$$

where the matrix $P=I_N-\varepsilon\mathcal{L}$ is called Perron matrix, $b_x$ is the linear deviation vector introduced during every update. $\Delta_x$ is the formation vector which contains the position data the follower should keep relative to leader. Perron matrix is right-stochastic, which satisfies $\sum_{j=1}^{N}p_{ij}=1,p_{ij}\geq 0,\forall i=1,2,...,N$. Two assumptions are founded on both fixed and dynamic topology cases to provide the sufficient convergence conditions. They are strictly proved in [21].

**Assumption 1.** *We set $\varepsilon\leq\frac{1}{d_{\max}+1}$. The non-diagonal elements of Perron matrix $p_{ij}$ equal to $\varepsilon$ (when $a_{ij}=1$) or 0 (when $a_{ij}=0$).*[1]

**Assumption 2.** *The topology has a directed spanning tree, and the formation tracking can be achieved asymptotically under the distributed control law* (2)*.*

### C. Observation Equation

In reality, observation through sensors has non-negligible noise. Thus, the observation equation is

$$z_x(t_k)=Cx(t_k)+\mu r(t_k) \tag{5}$$

where $z_x(t_k)$ is the observation vector of $x(t_k)$, $\mu$ is noise tunning parameter, and $C$ is the observation matrix. Without loss of the generality, we assume the noise vector $r(t_k)$ are zero-mean with $\text{Cov}(r(t_k))=I_N$. Every entity of $r(t_k)$ is a gaussian distribution at time $t_k$. From (4)-(5), to simplify the discussion, we set $C=I_N$, and the observation equation is

$$\begin{aligned}z_x(t_{k+1})&=Pz_x(t_k)+b_x+\mu r(t_{k+1})-\mu Pr(t_k)\\&=Pz_x(t_k)+b_x+q(t_{k+1}),\end{aligned} \tag{6}$$

where $q(t_{k+1})$ is total noise item. Equation (6) reveals a linear transition relation between $z_x(t_k)$ and $z_x(t_{k+1})$.

[1]This assumption is commonly used [6], [13], and can be relaxed in our scenario. $\hat{P}$ is not influenced by whether $P$ is weight matrix or not. $d_{max}$ is the maximum in-degree of all the robot nodes.

*D. Problem of Interest*

As shown in Fig. 1, topology inference center (TIC) retrieves the underling network structure of the formation control systems via observing the robots' trajectories without intervening system communication links or internal entity.

In this paper, we discuss the topology inference problem for networks of formation robots with directed information flow under link failure and creation (i.e., dynamic network topology). The following discussion will first address the inference problem in fixed topology and then solve the dynamic topology case based on the solution proposed for fixed one.

## III. Network Topology Inference Algorithms

*A. Sampling and Inference Mechanism*

The location of agent $i$ is $p_i = [x_i \ y_i]^T$ and updated every period of control time $T_c$. $T_c$ is fixed, small and therefore leads to the smooth motion trajectory. For TIC, the sampling period is denoted as $T_s$, and $T_s = T_c = t_{k+1} - t_k$. At every sampling time $t_k$, sensors of TIC sense locations of moving robots $p_{io} = [z_{ix} \ z_{iy}]^T$. After sequential samplings, we obtain the sampled feasible trajectory dataset as follows

$$\mathcal{D} = \left\{ \bigcup_{i \in V} (z_{ix}(t_k), \ z_{iy}(t_k))^T, k = 0, 1, \cdots n \right\}, \quad (7)$$

where $V = \{1, 2, \cdots, N\}$ is nodes' number set. Let $\mathcal{D} = \mathcal{D}_x \cup \mathcal{D}_y$, where $\mathcal{D}_x$, $\mathcal{D}_y$ are trajectory datasets of robots in x-axis and y-axis, and can be used for inference independently.

Under the equation (6), the noise vector $q(t_{k+1})$ contains $N$ components and they have the same distribution. The standard variance of $q_i(t_{k+1})$ is strictly restricted in Theorem 1.

**Theorem 1.** *Under* (6)*, the standard variance,* $\delta_i$*, of noise component* $q_i(t_{k+1})$ *is bounded in* $\left[\sqrt{\frac{N+1}{N}}\mu, \sqrt{2}\mu\right)$.

*Proof:* The $i$-th noise component $q_i(t_{k+1})$ contains two noise items as follows

$$\begin{aligned} q_i(t_{k+1}) &= \mu(r_i(t_{k+1}) - P_i r(t_k)) \\ &= \mu(r_i(t_{k+1}) - \sum\nolimits_{j=1}^{N} p_{ij} r_j(t_k)), \end{aligned} \quad (8)$$

where $P_i$ is the $i$-th row vector of Perron matrix, $r_i(t_k)$ is a gaussian noise with mean zero and variance one. The mean of noise $q_i(t_k+1)$ is represented as $\upsilon_i$, then $\upsilon_i = \mathbb{E}[\mu(r_i(t_{k+1}) - \sum_{j=1}^{N} p_{ij} r_j(t_k))] = \mu\mathbb{E}[r_i(t_{k+1})] - \sum_{j=1}^{N} p_{ij}\mathbb{E}[r_j(t_k)] = 0$. The standard variance is $\delta_i$ and $\delta_i^2 = \mathbb{E}[(q_i(t_{k+1}) - \bar{q}_i(t_{k+1}))^2]$. For $\bar{q}_i(t_{k+1})) = 0$, then $\delta_i^2 = \mathbb{E}[(q_i(t_{k+1}))^2]$. $q_i(t_{k+1})$ is the sum of independent and identically distributed noise $r_i(t_k)$,

$$\begin{aligned} \delta_i^2 &= \mu^2(\mathbb{E}[r_i^2(t_{k+1})] + \sum\nolimits_{j=1}^{N} p_{ij}^2 \mathbb{E}[r_j^2(t_k)]) \\ &= \mu^2(1 + \sum\nolimits_{j=1}^{N} p_{ij}^2). \end{aligned} \quad (9)$$

Thus, $\delta_i = \mu\sqrt{1^2 + \sum_{j=1}^{N} {p_{ij}}^2}$, which satisfies the inequality of arithmetic and geometric means

$$\mu\sqrt{1 + \frac{(\sum_{j=1}^{N} p_{ij})^2}{N}} \le \delta < \mu\sqrt{1^2 + (\sum\nolimits_{j=1}^{N} p_{ij})}^2. \quad (10)$$

For $\sum_{j=1}^{N} p_{ij} = 1, \forall i = 1, 2, ..., N$, and $p_{ij} \ge 0$, then the $\delta_i$ is strictly restricted in $\left[\sqrt{\frac{N+1}{N}}\mu, \sqrt{2}\mu\right)$. ■

Theorem 1 shows that the noise is bounded and the deviation caused will not accumulate with iterations for the noise is not time-variant. The amplitude-restricted noise ensures the following topology learning mechanism's feasibility.

It is apparent that the interaction topology of robot nodes is buried in the $P$ matrix in (6). Thus, the question is converted to a system identification problem that how to design a mechanism to identify $P$ using the feasible dataset $\mathcal{D}$.

Suppose we have got the estimated $\hat{P}$, then the adjacency matrix $\hat{A}$ corresponding to specific topology $\mathcal{G}(\hat{A})$ can be extracted from $\hat{P}$ [13], which is described by the following judging criteria

$$\hat{a}_{ij} = \begin{cases} 1, & \text{if } \hat{p}_{ij} \ge \tau, i \ne j \\ 0, & \text{if } \hat{p}_{ij} < \tau, i \ne j, \end{cases} \quad (11)$$

where $\tau$ is an nonnegative threshold. The threshold method requires repeated parameter adjustment of $\tau$, and beyond this, unsupervised k-means clustering algorithm warrants reflection. ultimately, the topology $\mathcal{G}(\hat{A})$ is derived and output.

*B. Directed Fixed Topology Inference*

Equation (4) shows that the formation control model is a multiple input multiple output (MIMO) linear system. We decomposes the system from MIMO to $N$ multiple input single output (MISO) systems in which parameters can be identified by $l_2$-norm minimum least square algorithm ($l_2$-LS).

Node $i$'s dynamic equation in x-axis is given by

$$z_{ix}(t_{k+1}) = z_x(t_k)^T P^i + b_{ix} + q_i(t_{k+1}), \quad (12)$$

where $P^i = [\ p_{i1} \ \ p_{i2} \ \ \cdots \ \ p_{iN}\ ]^T$ is the transpose of $i$'th row vector of Perron matrix $P$ that needs to be identified, and $z_x(t_k) = [\ z_{1x}(t_k) \ \ z_{2x}(t_k) \ \ \cdots \ \ z_{Nx}(t_k)\ ]^T$ is the observation vector at $t_k$. TIC observes $L$ times of iterations during formation tracking progress. We get $L$ equations at time $t_1, t_2, ..., t_L$. Hence, we combine the $L$ equations as follows

$$Z_{iL} = H_{L-1} P^i + b_{iL} + q_{iL} = T_{L-1} P^{i*} + q_{iL}, \quad (13)$$

where $Z_{iL} = [\ z_{ix}(t_1) \ \ z_{ix}(t_2) \ \ \cdots \ \ z_{ix}(t_L)\ ]^T$ is the robot $i$-th x-axis location data at time $t_1, t_2, ..., t_L$, and $q_{iL} = [\ q_i(t_1) \ \ q_i(t_2) \ \ \cdots \ \ q_i(t_L)\ ]^T$ is the noise vector introduced. $P^{i*} = [\ b_{ix} \ \ p_{i1} \ \ p_{i2} \ \ \cdots \ \ p_{iN}\ ]^T = [b_{ix} \ P^i]$ is the $N+1$ dimensional vector. The data matrix $T_{L-1}$ is the $L \times (N+1)$ matrix containing $N$ robot nodes' locations from $t_0$ to $t_{L-1}$. The goal of TIC is to find the most suitable row parameter vector $P^{i*}$ that minimize the quadratic cost function

$$\mathcal{J}(P^{i*}) = \sum_{k=1}^{L} \left(z_{ix}(t_k) - z_x(t_{k-1})^T P^i - b_{ix}\right)^2. \quad (14)$$

To prevent the influence of data which has severe deviation and prevent overfitting. We introduce the $l_2$-norm regulation item and we solve the optimization problem as follows

$$\hat{P}^{i*} = \underset{P^{i*}}{\arg\min}\, \mathcal{J}(P^{i*}) + \frac{\lambda}{2}\left\|P^{i*}\right\|^2 \ (\lambda \ge 0). \quad (15)$$

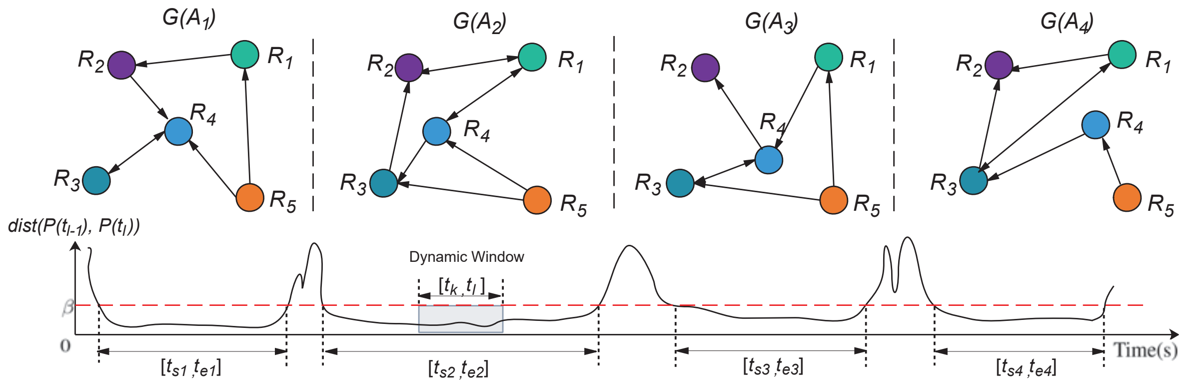

Fig. 2: Illustration of directed dynamic topology inference during the formation process.

Minimizing with respect to $\hat{P}^{i*}$, the optimal analytic solution of estimated parameter vector $\hat{P}^{i*}$ is written as

$$\hat{P}^{i*} = (T_{L-1}^T T_{L-1} + \lambda I_{N+1})^{-1} T_{L-1}^T Z_{iL}. \tag{16}$$

For equation (16), TIC does $N$ times of optimizations like (14) and the estimated Perron matrix is written as $\hat{P}^* = \begin{bmatrix} (\hat{P}^{1*})^T & (\hat{P}^{2*})^T & \cdots & (\hat{P}^{N*})^T \end{bmatrix}^T$. Then the final form

$$\hat{P}^* = T_L T_{L-1} (T_{L-1}^T T_{L-1} + \lambda I_{N+1})^{-1}, \tag{17}$$

where $T_L = \begin{bmatrix} Z_{1L} & Z_{2L} & \cdots & Z_{NL} \end{bmatrix}^T$ is the $N \times L$ data matrix of $N$ nodes from the first iteration at $t_1$ to the $L$-th iteration at $t_L$. $\hat{P}^* = [\hat{b}_x \ \hat{P}]$ is a block matrix, and $\hat{P}$ is the right block of $\hat{P}^*$. The following theorem gives conditions on which $l_2$-LS approach has optimal estimation in the sense of the least square estimation error. We present Algorithm 1 for $P$ estimation and $A$ extraction in directed fixed topology case.

**Theorem 2.** *Under* (17)*, when $L < N$, the number of equations is less than the number of parameters, $P$ can't be uniquely determined. When $E_{iL} = 0, L = N$, $P$ is uniquely determined, and when $E_{iL} \neq 0, L > N$, the optimal estimation $\hat{P}$ in the sense of least squares exists.*

### *C. Directed Dynamic Topology Inference*

Considering that the communication topology is time-variant and dynamic changing for package loss or the environmental interference, $P$ and $b_x$ are time-variant. For a stable inference, an assumption is made as follows:

**Assumption 3.** *In this dynamic changing case, each topology maintains a sufficient times of iterations $T_m, m \in N^*$. The TIC's observation times $L$ satisfies $N < L < \min\{T_m\}$.*

Based on the assumption above, there are mainly three key issues to be addressed when topology is dynamic: i) the trajectory data set $\mathcal{D}$ contains data belonging to different graph. A time slicing mechanism that recognizes the switching time and divides the data into different time slices belonging to various graphs is required. ii) the approach to sufficiently use the subset $\mathcal{D}_s$ of $\mathcal{D}$ for linear regression learning. iii) the robust mapping between graph $\mathcal{G}$ and linear regression result $\hat{P}$ in each slice. We next discuss the three solutions.

**Algorithm 1:** $l_2$-LS linear learning algorithm

**Input** : robots' trajectory dataset $\mathcal{D}$ observed by TIC sensor, $\mathcal{D} = \mathcal{D}_x \cup \mathcal{D}_y$;
**Output**: The topology graph $\mathcal{G}(\hat{\mathcal{A}})$;

1 Observe and get the number of robots $N$. Then, robots are labeled by set $\{1, ..., N\}$, set adjusted regulation parameter $\lambda$, combination weight $\alpha = 0.5$;
2 Choose the time slice $[t_s, t_e], (e - s = L > N)$ from $\mathcal{D}$, which is sufficient long for linear regression;
3 Make the estimation of $\hat{P}_x$, $\hat{P}_y$ using equation (15) with the trajectory dataset $\mathcal{D}_x$ and $\mathcal{D}_y$ in time slice $[t_s, t_e]$;
4 Figure out the $\hat{P} = \alpha \hat{P}_x + (1-\alpha)\hat{P}_y$;
5 Extract $\hat{A}$ from $\hat{P}$ using k-means algorithm;
6 **return** topology graph $\mathcal{G}(\hat{\mathcal{A}})$;

*1) Time Slicing:* As shown in the Fig. 2, from topology $\mathcal{G}_1$ to $\mathcal{G}_4$, each topology maintains a sufficient long period $[t_{s1}, t_{e1}], [t_{s2}, t_{e2}], [t_{s3}, t_{e3}], [t_{s4}, t_{e4}]$. We denote the $m$-th switching time as $t_{cm}$, and we know that $t_{cm} \in [t_{em}, t_{s(m+1)}], \forall m \in \{1, 2, 3\}$. It is obvious that during the time period $[t_{sm}, t_{em}], \forall m \in \{1, 2, 3, 4\}$, the estimation of Perron matrix $\hat{P}$ using any time slices $[t_k, t_l] \subseteq [t_{sm}, t_{em}], l - k = L > N$ is close to the true $P$ because of no interference data introduced from other topology's time period. That means the error curve depicting the distance between $\hat{P}$ and $P$ (defined as $dist(P, \hat{P})$ in Definition 1) is stable and close to zero in this case. On the contrary, if we choose a subset $\mathcal{D}_s$ of $D$ in $[t_k, t_l]$ for linear regression and $dist(P, \hat{P}) > \beta$ ($\beta$ is a threshold which judge whether the distance is close zero or not), then there must be one switching time $t_{cm} \in [t_k, t_l]$, and the switching serial number $m = j$ if $t_k \in [t_{sj}, t_{ej}]$. Here we define the distance between $\hat{P}$ and $P$. The definition is

**Definition 1.** *Define the distance function $dist(\cdot, \cdot)$, then the distance between $\hat{P}$ and true $P$ is written as*

$$dist(P, \hat{P}) = \frac{2}{N(N-1)} \sum_{i,j \in V, i<j} |\hat{p}_{ij} - p_{ij}|. \tag{18}$$

Under the evaluation criteria above, we have explained the principle of identifying switching time and dividing $\mathcal{D}$ into time slices. However, how to choose the subset $\mathcal{D}_s$ of $D$ in $[t_k, t_l]$ for regression is still a question to be solved. We next explain the dynamic window approach to solve the problem.

*2) Dynamic Window:* We suppose that the dataset $\mathcal{D}$ has the total time interval $[t_0, t_n]$. The dynamic window is initialized as a time queue $q = [t_k, t_l], l-k = L > N$. At the beginning, we set $t_k = t_0$ and get the estimation $\hat{P}(t_l)$ by doing the linear regression using $l_2$-LS from $\mathcal{D}_s$ in $q$. Then the window moves forward one step, the $q$ is updated by $q = [t_{k+1}, t_{l+1}]$, and we get the estimation $\hat{P}(t_{l+1})$ from the newly updated $\mathcal{D}_s$ in $q$. We continue the dynamic window sliding until we get the final estimation $\hat{P}(t_n)$. Totally, we get $n-L+1$ times of estimations of $P$ when the dynamic window is finished. The estimations can be written as $\hat{P}(t), t \in [t_L, t_n]$. Based on the estimations of $P$, the distance $dist(\hat{P}(t), P_m), t \in [t_L, t_n], m \in N^*$ is calculated for the time slicing mechanism proposed above.

*3) Graph Mapping:* Graph mapping refers to the mapping of $\mathcal{G}(\hat{P}(t)), \forall t \in [t_L, t_n]$ to a stable and robust topology graph $\mathcal{G}_m = \mathcal{G}(P_m)$. The distance curve $dist(\hat{P}(t), P_m)$ is discussed above to demonstrate that any one stable period corresponds to one topology period. However, from the standpoint of TIC, TIC can not calculate the $dist(\hat{P}(t), P_m)$ for the unknown $P_m$. To solve the problem, we choose the gradient of $\hat{P}(t)$ instead of $dist(\hat{P}(t), P_m)$ to do the time slicing. We find that the gradient curve $dist(\hat{P}(t_l), \hat{P}(t_{l+1}))$ has obvious waveform jitter when topology is dynamic changing through simulation.

Combining the three solutions proposed, we get the algorithm named as dynamic window least square algorithm (DWLS).

**Algorithm 2:** DWLS algorithm

**Input** : robots' trajectory datum $\mathcal{D}$ observed by TIC sensor, $\mathcal{D} = \mathcal{D}_x \cup \mathcal{D}_y$;
**Output**: The topology graph $\mathcal{G}(\hat{A}_m)$;

```
Observe the number of robots N. Robots are labeled by
  set {1, ..., N}, set adjusted regulation parameter λ,
  combination weight α = 0.5, error threshold β;
Time period of D is [t_0, t_n], and set regression time
  queue q = [t_k, t_l], l − k = L;
for t_k = t_0, t_l = t_L; t_l ≤ t_n; do
    Make the estimation of P̂_x, P̂_y using equation (15)
      with the D_x, D_y in period [t_k, t_l];
    P̂(t_l) = α P̂_x(t_l) + (1 − α) P̂_y(t_l);
    e(t_l) = dist(P̂(t_{l−1}), P̂(t_l)), m = 1, ∀l > L;
    if e1(t_l) ≤ β then
        if e(t_{l−1}) > β, m = m + 1;
        add t_l to queue [t_sm, t_em], m ∈ N*;
    else
        add t_l to queue [t_em, t_s(m+1)], m ∈ N*;
    end
end
Eliminate short time slice [t_sm, t_em], t_em − t_sm < L T_s
  and make m = m − 1 for the following slices in turn;
Choose the time slice [t_sm, t_em] from D_x, D_y for linear
  regression and get the final estimation which is combined
  as P̂_m = α P̂_mx + (1 − α) P̂_my;
Extract Â_m from P̂_m using k-means algorithm;
return the time slice of each topology [t_sm, t_em],
  switching time slices [t_em, t_s(m+1)], and sequential
  topology graphs G(Â_m);
```

## IV. Performance Evaluation

In this section, we first apply the consensus based formation control strategies to five robots. The leader's moving trajectory is an circle. We then present the inference results of $l_2$-LS and DWLS. The EAA which evaluates the performance of two algorithms is defined as:

**Definition 2.** *EAA is the index that presents the correct ratio of edges when comparing extracted $\hat{A}$ with true $A$.*

$$EAA = 1 - \frac{\sum_{j=1}^{N} \sum_{i=1, i \neq j}^{N} |\hat{a}_{ij} - a_{ij}|}{N(N-1)}. \tag{19}$$

### *A. Fixed Topology Case*

In this case, five mobile robots are required to preserve a pentagram formation (Fig. 3a). The formation error is shown in Fig. 3b. We set formation system's parameters $T_c = \varepsilon = 0.2$, and the TIC's observation and regression parameters $T_s = 0.2, \lambda = 0.01, \mu = 0.05, \alpha = 0.5$. TIC observes the process of formation including the formation forming stage $(0-5s)$ and formation keeping stage $(5-80s)$. $l_2$-LS algorithm does inference using $\mathcal{D}$ $(L = 400)$. In Fig. 3c, we display the off-diagonal entries of the true Perron matrix with black dots and the estimated ones with green dots. The matrix has been vectorized by means of column-major ordering, and the (vectorized) $(i, j)$ pairs have been rearranged in such a way that the nonzero entries appear before the zero entries. After $P$ estimating, k-means algorithm is adopted to cluster the dots and extract matrix $\hat{A}$, the clustering result is in Fig. 3d.

It is shown that one entity of matrix $A$ is misidentified. The inference accuracy $EAA$ is 95.00%.

### *B. Dynamic Topology Case*

DWLS's inference parameters is $\beta = 0.5, L = 30$. The formation keeping stage $(5-80s)$ includes three topology changing points at $20s, 40s, 60s$ and four different topology maintaining periods $[0s, 20s], [20s, 40s], [40s, 60s], [60s, 80s]$. As Fig. 2 shows, the topology switches in the following order $\mathcal{G}_1 \rightarrow \mathcal{G}_2 \rightarrow \mathcal{G}_3 \rightarrow \mathcal{G}_4$. TIC also observes the whole process (n=400) and use DWLS to regress the Perron matrix with the dataset $(p_o(t_k), p_o(t_{k+1}), ..., p_o(t_l)), l-k = L = 30, k \in \{0, 2, \cdots, 370\}$. Totally, TIC will do $n-L+1$ times of computation and get $\hat{P}(t_l), l \in \{30, 21, \cdots, n\}$. Figure. 3e simulates the error distance $dist(\hat{P}(t_l), P_m), m \in \{1, 2, 3, 4\}$. Moreover, the distance $dist(\hat{P}(t_l), \hat{P}(t_{l+1}))$ which can be calculated by TIC is shown in Fig. 3f. It is clearly found that at the switching times, there are sharp rises and the severe turbulence will maintain a short time slot. Regressed Perron

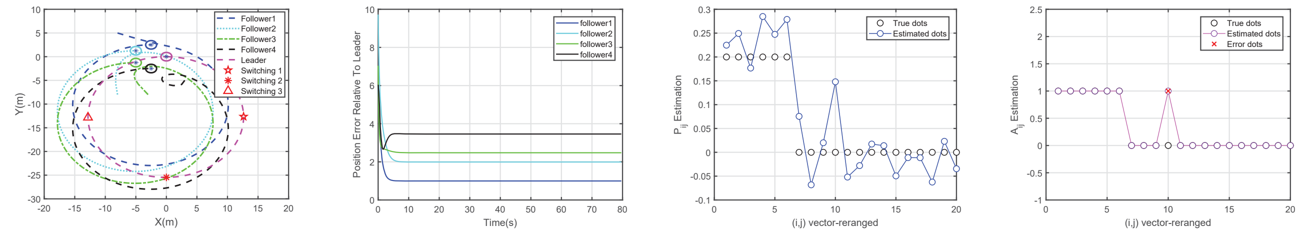


(a) Formation Trajectory (case 1-2). (b) Formation Error (case 1). (c) $\hat{P}$ Estimated (case 1). (d) $\hat{A}$ Extracted (case 1).

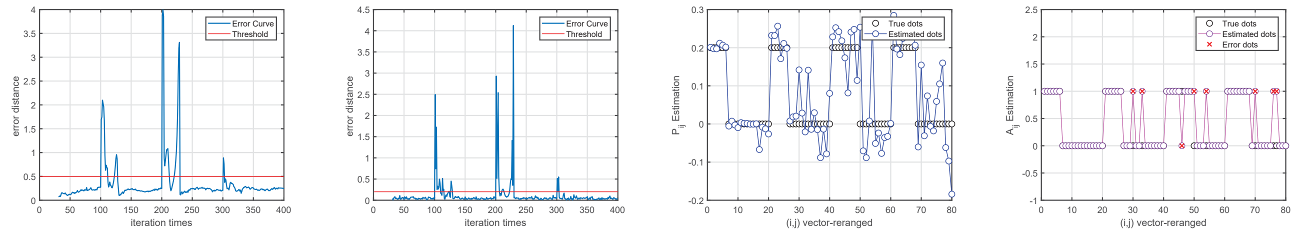


(e) Distance Curve Between $\hat{P}(t)$ and $P_m, m \in \{1, 2, 3, 4\}$ (case 2). (f) Distance Curve Between $\hat{P}(t_l)$ and $\hat{P}(t_{l+1})$)(case 2). (g) $\hat{P}$ Estimated (case 2). (h) $\hat{A}$ Extracted (case 2).

Fig. 3: Simulation results of formation control of five holonomic robots and topology inference performance in fixed topology (case 1) and dynamic topology (case 2). The parameters are set as $T_c = T_s = \varepsilon = 0.2, \mu = 0.05$, the running time is $80s$.

matrix using data in four topology maintaining slices are presented horizontally in Fig. 3g and $\hat{A}$ extracted by k-means is illustrated in Fig. 3h, which shows that only eight entities of matrix $A$ is misidentified and the accuracy is $90.00\%$.

## V. Conclusion

We investigate topology inference problem via observation for multi-robot formation control in this paper. Firstly, we propose an effective algorithm $l_2$-LS which transforms the topology inference issue into a linear regression problem. Then, to deal with the topology inference problem in dynamic topology case, we propose DWLS algorithm. The DWLS algorithm has three creative basics, that is dynamic window, time slicing and graph mapping. Finally, simulations demonstrate the effectiveness of these two algorithms.

## References


[1] Y. Q. Chen and Z. Wang, "Formation control: a review and a new consideration," in *2005 IEEE/RSJ International Conference on Intelligent Robots and Systems*. IEEE, 2005, pp. 3181–3186.

[2] Y. Feng, Z. Duan, W. Ren, and G. Chen, "Consensus of multi-agent systems with fixed inner connections," *International Journal of Robust and Nonlinear Control*, vol. 28, no. 1, pp. 154–173, 2018.

[3] K.-K. Oh, M.-C. Park, and H.-S. Ahn, "A survey of multi-agent formation control," *Automatica*, vol. 53, pp. 424–440, 2015.

[4] S. Zhu, L. Xie, C. Chen, and X. Guan, "Collective behavior of mobile agents with state-dependent interactions," *Automatica*, vol. 51, pp. 394–401, 2015.

[5] J. He, L. Cai, and X. Guan, "Preserving data-privacy with added noises: Optimal estimation and privacy analysis," *IEEE Transactions on Information Theory*, vol. 64, no. 8, pp. 5677–5690, 2018.

[6] A. Santos, V. Matta, and A. H. Sayed, "Local tomography of large networks under the low-observability regime," *arXiv preprint arXiv:1805.09081*, 2018.

[7] G. Mei, X. Wu, Y. Wang, M. Hu, J.-A. Lu, and G. Chen, "Compressive-sensing-based structure identification for multilayer networks," *IEEE Transactions on Cybernetics*, vol. 48, no. 2, pp. 754–764, 2017.

[8] J. He, P. Cheng, L. Shi, J. Chen, and Y. Sun, "Time synchronization in wsns: A maximum-value-based consensus approach," *IEEE Transactions on Automatic Control*, vol. 59, no. 3, pp. 660–675, 2013.

[9] S. Shahrampour and V. M. Preciado, "Topology identification of directed dynamical networks via power spectral analysis," *IEEE Transactions on Automatic Control*, vol. 60, no. 8, pp. 2260–2265, 2015.

[10] S. Boccaletti and V. Latora, "The structure and dynamics of complex networks," *International Journal of Bifurcation and Chaos*, vol. 17, no. 7, pp. 2195–2200, 2007.

[11] H.-J. Park and K. Friston, "Structural and functional brain networks: from connections to cognition," *Science*, vol. 342, no. 6158, p. 1238411, 2013.

[12] C. J. Quinn, T. P. Coleman, N. Kiyavash, and N. G. Hatsopoulos, "Estimating the directed information to infer causal relationships in ensemble neural spike train recordings," *Journal of Computational Neuroscience*, vol. 30, no. 1, pp. 17–44, 2011.

[13] V. Matta and A. H. Sayed, "Consistent tomography under partial observations over adaptive networks," *IEEE Transactions on Information Theory*, 2018.

[14] M. Tsitsvero, S. Barbarossa, and P. Di Lorenzo, "Signals on graphs: Uncertainty principle and sampling," *IEEE Transactions on Signal Processing*, vol. 64, no. 18, pp. 4845–4860, 2016.

[15] D. Materassi and M. V. Salapaka, "On the problem of reconstructing an unknown topology via locality properties of the wiener filter," *IEEE Transactions on Automatic Control*, vol. 57, no. 7, pp. 1765–1777, 2012.

[16] C. J. Quinn, N. Kiyavash, and T. P. Coleman, "Directed information graphs," *IEEE Transactions on Information Theory*, vol. 61, no. 12, pp. 6887–6909, 2015.

[17] J. Etesami and N. Kiyavash, "Measuring causal relationships in dynamical systems through recovery of functional dependencies," *IEEE Transactions on Signal and Information Processing over Networks*, vol. 3, no. 4, pp. 650–659, 2017.

[18] X. Dong, D. Thanou, P. Frossard, and P. Vandergheynst, "Learning laplacian matrix in smooth graph signal representations," *IEEE Transactions on Signal Processing*, vol. 64, no. 23, pp. 6160–6173, 2016.

[19] B. Pasdeloup, V. Gripon, G. Mercier, D. Pastor, and M. G. Rabbat, "Characterization and inference of graph diffusion processes from observations of stationary signals," *IEEE Transactions on Signal and Information Processing over Networks*, 2017.

[20] B. Pasdeloup, M. Rabbat, V. Gripon, D. Pastor, and G. Mercier, "Graph reconstruction from the observation of diffused signals," in *Communication, Control, and Computing (Allerton), 2015 53rd Annual Allerton Conference on*. IEEE, 2015, pp. 1386–1390.

[21] F. L. Lewis, H. Zhang, K. Hengster-Movric, and A. Das, *Cooperative control of multi-agent systems: optimal and adaptive design approaches*. Springer Science & Business Media, 2013.